

MECHANICAL LOADING EFFECTS ON THE RESISTIVITY OF THIN FILM SEMICONDUCTORS

Dennis Lange^{1,2}, Pere Roca i Cabarrocas¹, N. Triantafyllidis¹, D.Daineka²

1: Laboratoire de Mécanique des Solides/CNRS, Ecole Polytechnique, 91128 Palaiseau - France

2: Laboratoire de Physique des Interfaces et Couches Minces, CNRS, Ecole Polytechnique, 91128 Palaiseau - France

ABSTRACT: The influence of mechanical stress on PECVD thin film layers (250 to 500 nm) of hydrogenated amorphous and microcrystalline silicon (both intrinsic, p- and n-doped) as well as indium tin oxide (ITO) and aluminum doped zinc oxide (ZnO:Al) was examined via uniaxial tension and compression tests and a simultaneous measurement of the resistivity both parallel and perpendicular to the applied stress (piezoresistivity). The resistivity for intrinsic hydrogenated amorphous layers is increasing for tensile strain whereas it is decreasing for intrinsic hydrogenated microcrystalline layers. P-doped layers of microcrystalline silicon have an increasing resistivity with increasing tensile strain which is in opposition to the behavior of n-type layers that show a decrease in resistivity for the same strain. Both ITO and ZnO:Al show a strong increase in resistivity with strain. The experiments for every material type show that the effect is reversible up to a certain strain and that a permanent damage remains if the sample is subjected to a strain exceeding this limit. In-situ mechanical tests in a scanning electron microscope demonstrate that such irreversible changes are due to crack formation when a certain strain is exceeded. These cracks can be observed perpendicular to the direction of the applied stress.

Keywords: a-Si:H, μ -Si:H, ZnO, ITO, Electrical Properties

1 Introduction

Stress plays an important role in the performance of silicon solar cells. Firstly process steps in the fabrication of both wafer based silicon solar cells and thin film silicon solar cells can cause stresses in the final devices. Soldering is for instance a critical step in the processing of monocrystalline and polycrystalline cells [1, 2]. Plasma processes used for thin film deposition equally lead to non-negligible stresses [3, 4]. This can lead to numerous defects on different length scales that influence the device characteristics [5, 6]. Stress in silicon materials leads however also to a change in resistivity that has nothing to do with the formation of defects but rather with a change of crystal symmetry that causes a change of the electronic properties. This effect was first studied by Smith [7] and several works followed him that added a profound theoretical foundation [8, 9]. From the 90s on, this effect was beneficially used in transistors in form of strained silicon technology [10]. A mobility gain of up to 30% can be realized with a strain of just 0.2% in the case of mono-crystalline silicon [11]. Those methods are known as strain engineering [12].

Both theoretical and experimental works have shown that there is also a significant effect in amorphous and polycrystalline silicon layers, junctions and cells [13, 14, 15]. Zinc oxide, which serves as a transparent conductive oxide (TCO) in photovoltaic cells, shows as well a non-negligible change in resistivity with stress [16].

This work is a first step to evaluate if strain engineering could also be used in photovoltaic cells to enhance their characteristics. The influence of stress on every single layer in a typical pin thin film solar cell consisting of a transparent conductive oxide, a p-doped, an intrinsic and a n-doped layer (either microcrystalline or amorphous) was determined. This method will be expanded to solar cells in subsequent works.

2 EXPERIMENTALS

2.1 Layer deposition

The change in resistivity of a semiconducting layer (n-, p-doped and intrinsic hydrogenated amorphous (a-

Si:H) and microcrystalline silicon (μ -Si:H) plus aluminum doped zinc oxide (ZnO:Al) and indium tin oxide (ITO) with increasing strain was determined. In order to perform mechanical tests, a polyimide foil (PI) substrate (110 μ m and 50 μ m DuPont™ Kapton® films) was used. It was cleaned with deionized water, acetone and ethanol in an ultrasonic bath prior to depositions. All depositions of amorphous and microcrystalline layers were performed in a capacitively coupled radio-frequency (RF) PECVD reactor at 150°C. Amorphous layers were deposited at low pressure (0.1 torr), low RF power (7 mW/cm²) and no H₂ dilution whereas the microcrystalline layers were deposited at high pressure (1.7 torr), moderate RF power (70 mW/cm²) and with a H₂/SiH₄ ratio of 500/4 sccm. ZnO:Al layers were deposited via PVD with an argon flow of 30 sccm at a power of 250W whereas ITO layers were deposited at a argon/oxygen flow of 43/3 sccm and at a power of 200 W. A protective silicon nitride (SiN_x) barrier layer was deposited via electron cyclotron resonance (ECR) PECVD onto the PI substrate to prevent chemical interactions between the polyimide foil and the silicon layers during their subsequent PECVD deposition of the silicon layer. Rectangular aluminum contacts with a width of 1 cm and a distance of 1mm were provided via thermal evaporation.

2.2 Sample preparation and mechanical tests

It is necessary to glue the polyimide foil with the deposited layers onto a rigid PVC substrate in order to perform mechanical tests. This has the advantage that the sample is much easier to handle. The adhesive is an alkyl cyanoacrylate adhesive that is normally used for strain gauges and is thus elastic in the strain range examined (plus minus 1%). Several steps of surface preparation for the back surface of the polyimide foil and the front of the PVC substrate are necessary to guarantee a good adhesion. A roughening with sand paper is followed by cleaning with ethanol, an acidic solution and a basic solution (the 2 latter provided by the supplier of the adhesive). Wires are glued to the 2 rectangular aluminum contacts (10 mm x 5 mm, 1 mm distance) with a conductive epoxy adhesive. The whole configuration can

be seen in figure 1.

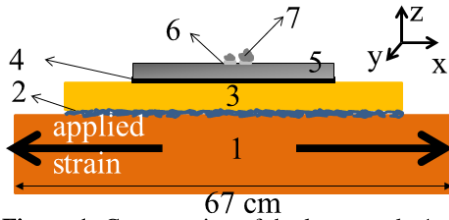


Figure 1: Cross section of the layer stack: 1: 5 mm thick PVD substrate, 2: alkyl cyanoacrylate adhesive, 3: 50 μm polyimide foil, 4: 150 nm SiNx, 5: semiconducting layer, 6: evaporated aluminum contacts, 7: conductive epoxy adhesive to attach wires.

The rectangular contacts (10 mm x 5 mm, 1 mm distance) are placed in such a way that the current is flowing either parallel (upper drawing, called A1 configuration) or perpendicular (lower drawing, called A2 configuration) to the applied strain as shown in Figure 2

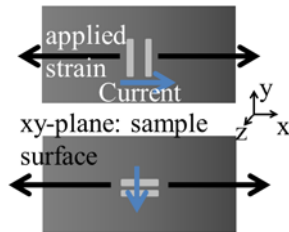


Figure 2: Schematic top view of the sample. The rectangular contacts (10 mm x 5 mm, 1 mm distance) are placed in such a way that the current is flowing either parallel (upper drawing, called A1 configuration) or perpendicular (lower drawing, called A2 configuration) to the applied strain.

The whole layer stack was then clamped to two high pressure clamps (to prevent any slippage) that were connected to a hydraulic press. The effective area to be deformed is 67 mm (width) x 10 mm (height). This is a compromise between experimental constraints (67 mm is the width of the clamps and a height less than 10 mm makes it difficult to contact the samples) and the wish to have a uniform uniaxial strain in x direction. This means that the ratio of the strain ϵ_{yy} to the strain ϵ_{xx} must be as close to 0 as possible. X, as can be seen in figure 1 and figure 2, is always to the direction of the applied stress and hence the main strain component. Simple linear elastic calculations with the finite element software Abaqus FEA were done to determine the ratio $\epsilon_{yy}/\epsilon_{xx}$ in the geometry described above. The calculated value of 0.02 is satisfyingly low and the above mentioned design was therefore used.

The specimens were then deformed to a certain displacement and the change in current was registered. A four point method was used to measure resistivity. The strain of the sample was measured via digital image correlation. To use this technique, black and white spray paint is applied between the contacts of the specimen to obtain a speckle pattern. A camera is then recording images during the experiment and the software Vic-2D[®] of Correlated SolutionsTM calculates the in-plane 2D stress tensor (ϵ_{xx} , ϵ_{yy} and ϵ_{xy}) based on the positional change of the speckles.

The same kind of experiment was repeated in-situ

in a scanning electron microscope chamber. The basic setup was exactly the same as for the atmospheric tests just that a special stage and a smaller press allowed for in-situ testing. The goal of this experiment was to see if a change in the IV-curve can be correlated directly to cracks or other signs of mechanical failure.

3 Results

3.1 Silicon layers

All examined layers so far show a significant change (at least a few percent) in resistivity as it can be seen in figure 3. Intrinsic materials show in general a larger relative change in resistivity than doped materials for a strain ϵ_{xx} of 0.5% (up to -20% and +30% in the case of $\mu\text{-Si:H}$ and a-Si:H and up to -15% and +20% in the case of n-doped $\mu\text{-Si:H}$ and p-doped $\mu\text{-Si:H}$). The sign (positive meaning an increasing resistivity) seems to depend on the material type and doping. The resistivity in the A2 configuration (the applied strain and current flow being perpendicular to each other) shows little change (see the p-doped $\mu\text{-Si:H}$ sample in figure 3 marked by a asterisk). This is a direct consequence of the sample design. The lateral contraction due to the Poisson effect would normally be in the range of 0.4 for the PVC substrate (it is safe to assume that the thin films follow the deformation of the thick substrate) and ϵ_{yy} would have a value of 0.2% for ϵ_{xx} being 0.5%. The high width/height ratio leads however as described before just to a very small lateral contraction ϵ_{yy} of -0.03% which still leads to a small change in resistivity.

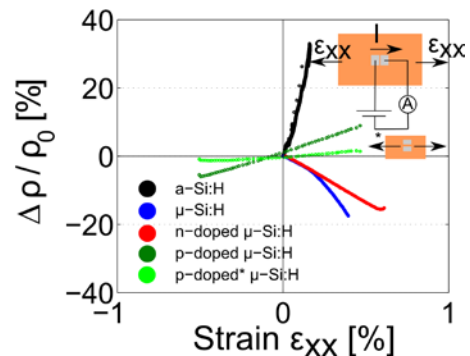


Figure 3: Relative change of resistivity as a function of the strain component ϵ_{xx} for silicon based materials

3.2 Transparent Conductive Oxides

By far the biggest sensitivity to strain in the A1 configuration is obtained for ITO and ZnO:Al as it can be seen in figure 4. Both curves show a hysteresis behavior. The change for ITO is up to 170% for a value of 0.5% for ϵ_{xx} . For the same strain, the change for ZnO:Al is more than 6000%. It must be noted that tiny changes in strain lead to huge changes in resistivity. As it can be seen in the lower part of the ITO curve in figure 4, a strain just slightly lower than 0.5% leads to considerably lower change in resistivity that is however reversible. The big changes beyond 0.5% strain just partly recover to the initial values.

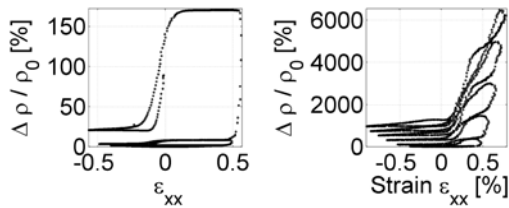


Figure 4: Relative change of resistivity as a function of the strain component ϵ_{xx} for indium tin oxide (left) and aluminum doped zinc oxide (right)

The behavior is however very different if the current flow and the applied strain are perpendicular to each other (A2 type experiment). Those results can be seen in figures 5 and figure 6. Shown are the strain parallel to the applied stress, ϵ_{xx} , (and thus perpendicular to the flowing current) and the strain perpendicular to the applied stress (and thus parallel to the current flow), ϵ_{yy} . The strain range for ϵ_{xx} is the same as for the experiments in the A1 configuration. The reasoning to explain the small change in resistivity is similar to the one for the p-doped μ -Si:H sample in figure 3. The decisive strain component is ϵ_{yy} because it is parallel to the current flow. Even if ϵ_{xx} is 0.5, ϵ_{yy} just reaches values of -0.08% which leads to little changes: nearly zero for ITO and just 150 % for ZnO:Al.

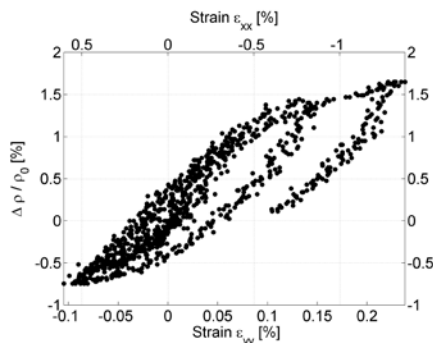


Figure 5: Relative change of resistivity as a function of the strain component ϵ_{xx} and ϵ_{yy} in the A2 configuration for ITO. The applied strain and the current are perpendicular to each other. The decisive strain component is thus the one parallel to the current flow: ϵ_{yy}

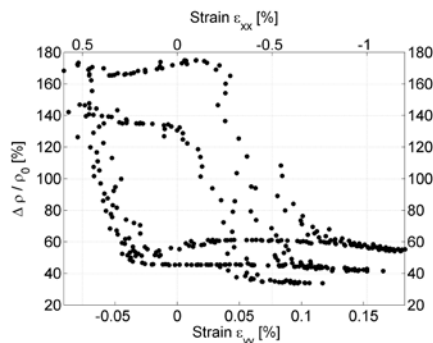


Figure 6: Relative change of resistivity as a function of the strain component ϵ_{xx} and ϵ_{yy} in the A2 configuration for ZnO:Al. The applied strain and the current are perpendicular to each other. The decisive strain component is thus the one parallel to the current flow: ϵ_{yy}

3.3 Cycling

In cyclic testing, samples were subjected to a certain strain for 50 cycles before the strain was slightly

increased to deform the sample again for 50 times. These experiments were only done in the tensile regime. Figure 7 depicts the results for a n-doped μ -Si:H sample. There are two strain regimes observable. Up to a certain strain, the strain-resistivity behavior is repeatable and the resistivity returns to its original value after every deformation cycle. If the same sample is however subjected to a certain critical strain, a huge increase in the resistivity value is observable and the resistivity does not fully recover. It does however stabilize after a few cycles. This can be linked qualitatively to the appearance of cracks perpendicular to the applied strain as depicted by figure 8 which is showing a SEM image of an in-situ mechanical test with simultaneous current measurement. The cracks marked by red circles could be observed when the current was abruptly increasing as observable in the right graph of figure 7. It could be observed that the cracks close partly during unloading but never completely, which may explain why the current value does not return to its starting value. The appearance of cracks perpendicular to the applied strain might also explain why the current in A2 experiments is only little affected by strain. The cracks in this case are parallel to the current flow which means that electrons have still an unaffected path to flow to the other contact.

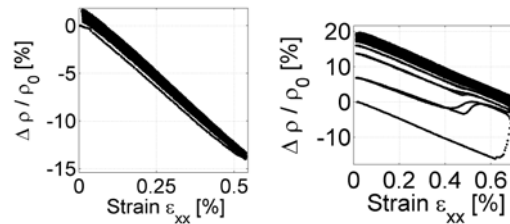


Figure 7: Cyclic testing on a n-doped μ -Si:H sample

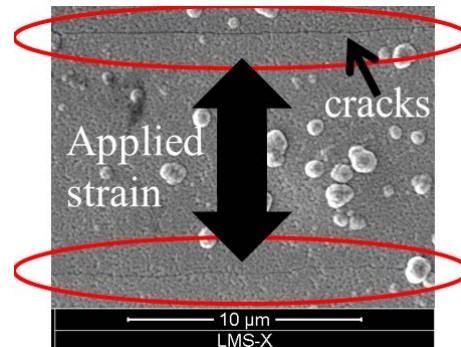


Figure 8: In-situ SEM image during the mechanical stressing of a n-doped μ -Si:H. The resistivity is measured simultaneously. Cracks are visible after applying a tensile strain of X%.

4 DISCUSSION AND FUTURE WORK

The goal of this study was to identify to what extent the layers in a thin film photovoltaic PIN solar cell stack are sensitive to strain and eventually identify the limiting ones. It turns out that all layers are considerably sensitive to strain and that this is especially true for the two transparent conductive oxides (ITO and ZnO:Al) that were tested. The sensitivity to strain was to be expected in the case of silicon materials as its piezoresistive behavior is well documented [7,13]. Far larger is however the effect for ITO and ZnO:Al. This is however just true if current flow and applied strain are parallel to each other. If this is not the case, the current is mostly

unaffected as it can be seen in figure 5 and figure 6. The direction of the main strain component (meaning the strain component parallel to the applied stress) and the current flow with respect to each other plays a decisive role.

For future work this means that the out-of-plane resistivity has to be measured with respect to a stress applied parallel to the surface. This is a case closer to a real photovoltaic cell and might cause even other effects because the distance between the contacts is reduced to the a few hundred nanometers.

From a materials point of view, monocrystalline silicon will also be considered in future experiments because it is most likely to exhibit the biggest effect of all silicon materials.

5 SUMMARY

Thin-film semiconductors (intrinsic and doped hydrogenated amorphous and microcrystalline silicon plus indium tin oxide and aluminum doped zinc oxide) deposited on flexible polyimide substrates were subjected to a controlled mechanical strain while the change in material resistivity measured.

The change in resistivity for silicon ranges from 10 to 40% for 0.5% strain. Intrinsic layers show in generally a bigger change than doped layers. The sign of the change (increase or decrease in resistivity) depends both on the material and doping type.

Transparent conductive oxides show by far the biggest changes of 150% for 0.5% strain in the case of ITO and 6000% in the case of aluminum doped zinc oxide.

Cycling tests on a n-doped hydrogenated microcrystalline silicon sample show that a strain of up to 0.5 % can be withstand repeatedly but that surpassing this limit leads to a permanent increase in resistivity. In-situ mechanical tests in a SEM chamber reveal that this is most likely due to the formation of cracks.

6 REFERENCES

- [1] Wendt, J., Träger, M., Mette, M., Pfennig, A., Jäckel, B., Proceedings 24th European Photovoltaic Solar Energy Conference (2009) 3420.
- [2] Gabor, A. M., Ralli, M., Montminy, S., Alegria, L., Bordonaro, C., Woods, J., Williams, T., Proceedings 21st European Photovoltaic Solar Energy Conference (2006) 4
- [3] Y. Fu, J. Luo, S. Milne, A. Flewitt and W. Milne, Materials Science and Engineering B 124-125 (2005) 132
- [4] C. Iliescu, M. Avram, B. Chen, A. Popescu, V. Dumitrescu, D. P. Poenar, A. Sterian, D. Vrtacnik, S. Amon, P. Sterian, Journal of Optoelectronics and Advanced Materials 13 (2011) 387
- [5] Sarau, G.; Bochmann, A; Christiansen, S.; Schönfelder, S., 35th IEEE Photovoltaic Specialists Conference 2010
- [6] He, S. and Danyluk, S. and Tarasov, I. and Ostapenko, S., Applied Physics Letters, 89, 111909 (2006)
- [7] C. S. Smith, Physical Review 94,1(1954) 42
- [8] C. Herring, E. Vogt, Physical Review 101,3 (1956) 944
- [9] J. Bardeen, W. Shockley, Physical Review 80,1(1950) 72
- [10] E. Parton and P. Verheyen, III-Vs Review 19,3 (2004) 8
- [11] S. E. Thompson,, M. Armstrong, C. Auth, S. Cea, R. Chau, G. Glass,T. Hoffman, J. Klaus, Z. Ma, B. McIntyre, A. Murthy, B. Obradovic, L. Shifren, S. Sivakumar, S. Tyagi, T. Ghani, K. Mistry, M. Bohr, Y. El-Mansy,IEEE Elecctron Device Letters 25,4 (2004) 191
- [12] Li, J., Shan, Z., Ma, E., MRS Bulletin 39, 2. (2014)
- [13] P. French and A. Evans, Electronics Letters 20, 24 (1984) 999
- [14] R. Jones, T. Johnson, W. Jordan, S. Wagner, J. Yang, S. Guha, IEEE Photovoltaic Specialists Conference (2002) 1214
- [15] J. Creemer, F. Fruett, G. Meijer, IEEE Sensors Journal 1, 2 (2001) 98
- [16] Chen, Q., Sun, Y., Wang, Y., Cheng, H., & Wang, Q.-M. (2013), Sensors and Actuators A: Physical 190, (2013) 161